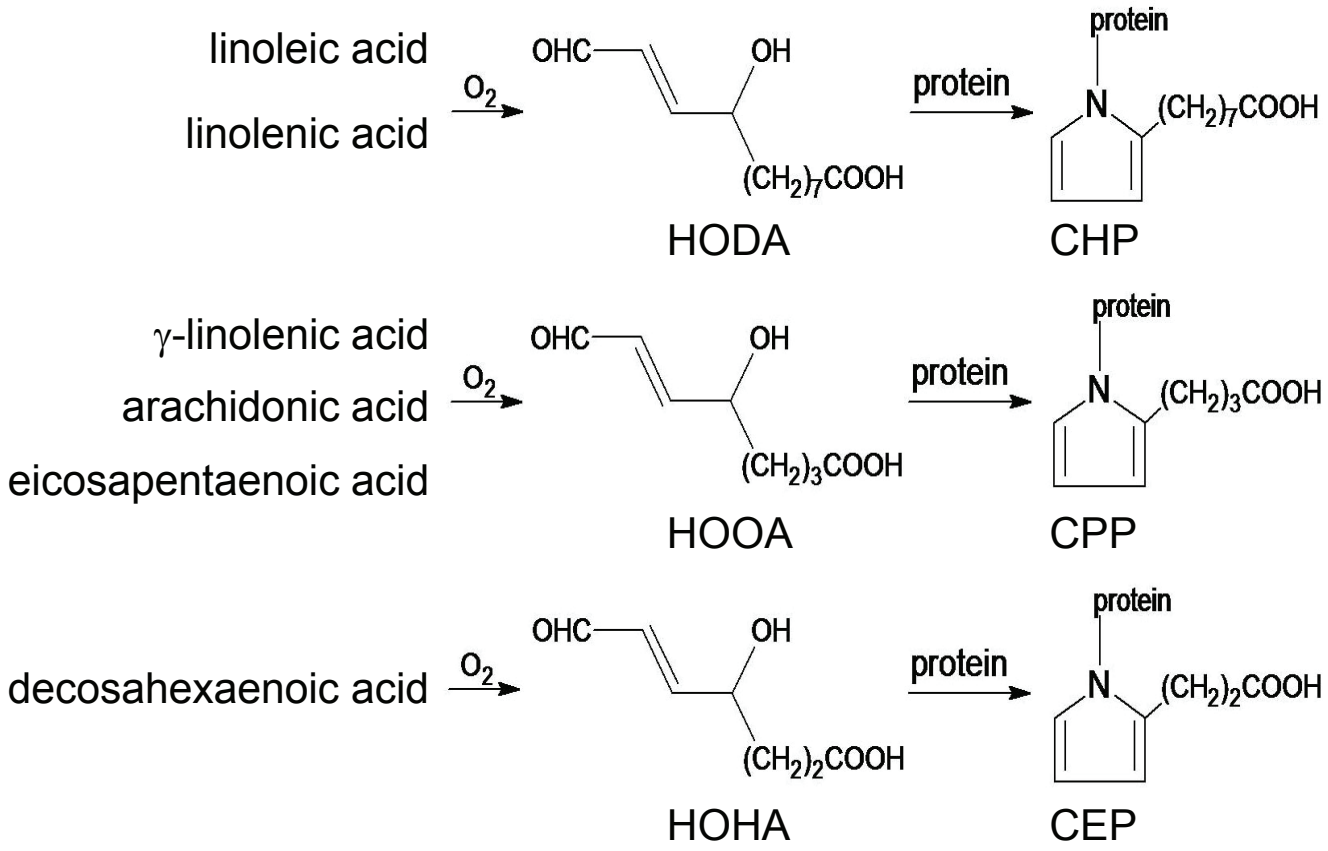

Fig.S1. Schematic diagrams of carboxyalkylpyrrole protein adduct (CAP) biogenesis.
HODA - 9-hydroxy-12-oxododec-10-enoic acid;
HOOA - 5-hydroxy-8-oxooct-6-enoic acid;
HOHA - 4-hydroxy-7-oxohept-5-enoic acid;
CHP - 2-(ω-carboxyheptyl) pyrrole;
CPP - 2-(ω-carboxypropyl)pyrrole;
CEP - 2-(ω-carboxyethyl)pyrrole.

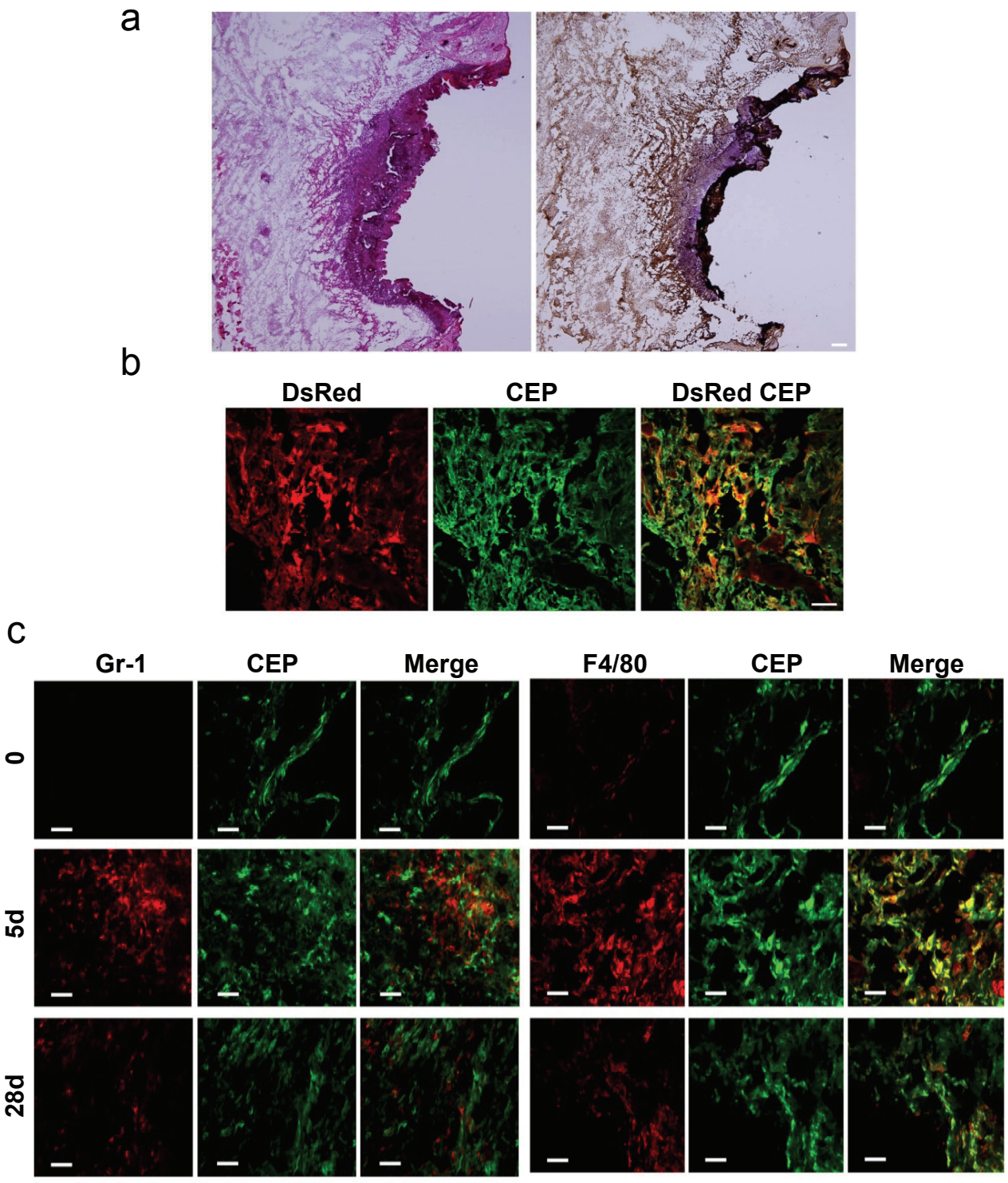

Fig.S2. CEP is accumulated in wounded areas. **a.** Left - H&E staining of wound tissue collected 3 days after injury. Right – CEP immunostaining of the same wound; scale bar is 100 μm. **b.** CEP (green) is present in bone marrow derived cells (red). Wound tissue was collected 5 days after injury from mice transplanted with bone marrow from DsRed expressing mice; scale bar is 50 μm. **c.** Co-staining for Gr-1 (red), F4/80 (red) and endogenous CEP (green) in wound tissues before injury (0), 5 and 28 days after injury as indicated; scale bars are 40 μm.

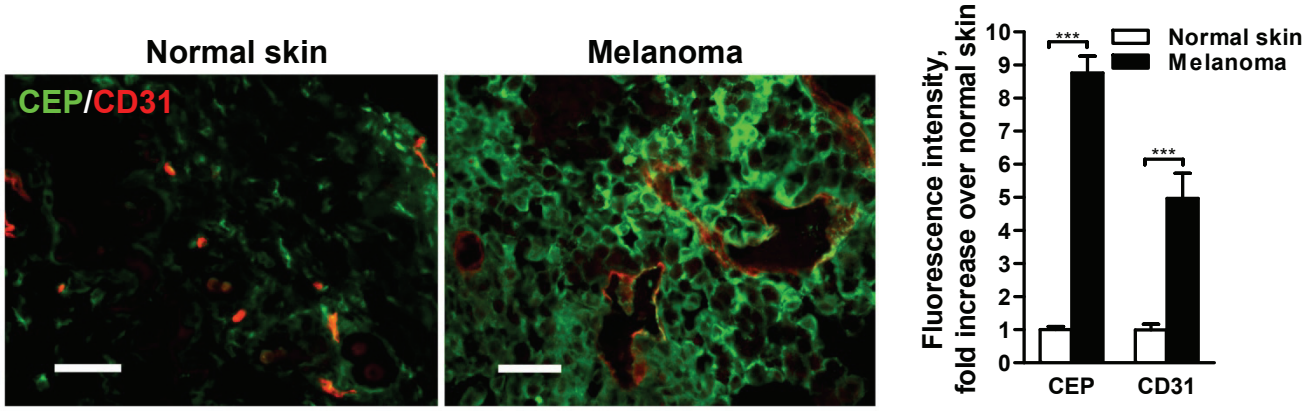

Fig.S3. Co-staining for CEP (green) and CD31 (red) in implanted mouse B16-F10 melanoma and normal skin of C57BL/6 mice as shown; scale bars are 40 μm. Right- Quantifications of CEP intensity and vascularization (based on CD31 staining). Bars represent fold increase over control (normal skin), mean ± s.e.m., n=5. *** represents $p<0.001$ vs. normal skin.

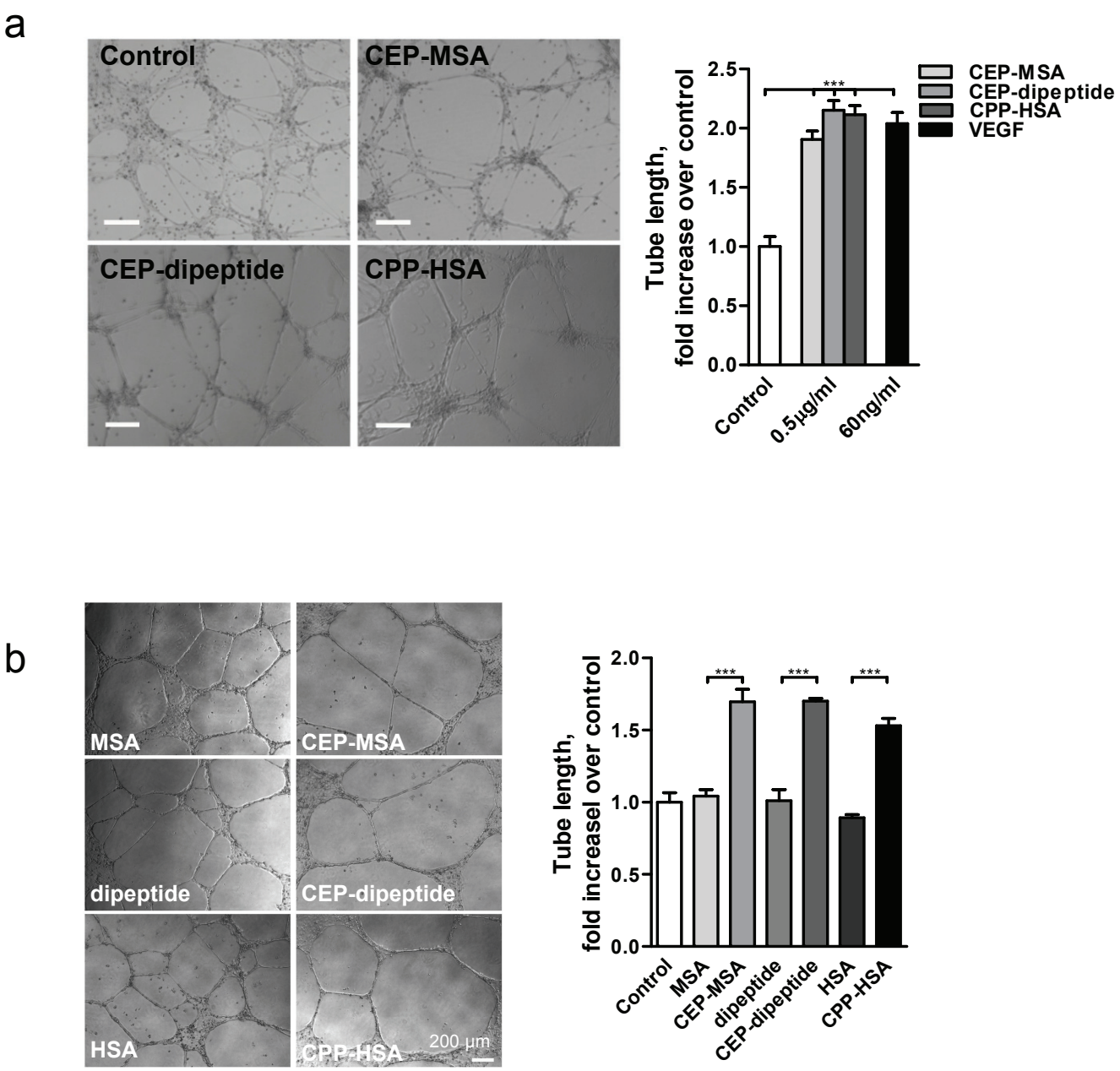

Fig.S4. The pro-angiogenic effect of oxidized adducts is not restricted to a particular source of endothelial cells. **a.** Mouse Lung Microvascular EC (MLEC) tube formation assay: Left- representative micrographs of control (no treatments) and CEP-MSA, CEP-dipeptide and CPP-HSA treated cells; scale bars are 200 µm. Right- quantification of tube formation assay (VEGF as positive control) as indicated. Bars represent fold increase over control, mean ± s.e.m., n=4. *** represents $p<0.001$. **b.** HUVEC tube formation assay: Left- representative micrographs of cells treated with CEP-MSA, CEP-dipeptide and CPP-HSA or unmodified proteins as indicated; scale bar is 200 µm. Right- quantification of tube formation assay in the presence of CEP adducts or unmodified proteins. Bars represent fold increase over untreated control, mean ± s.e.m., n=5. *** represents $p<0.001$ vs. control.

a

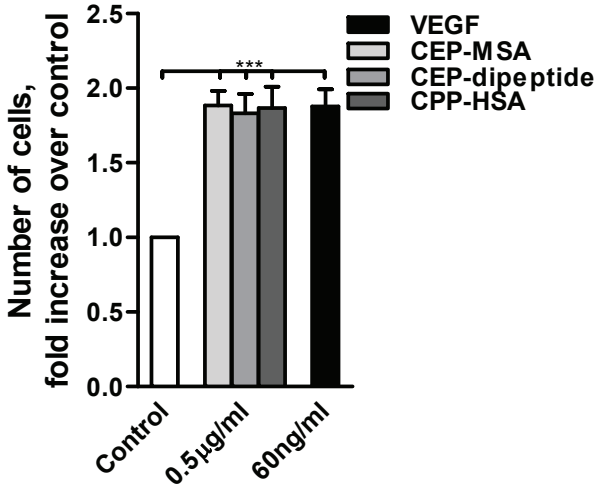

b

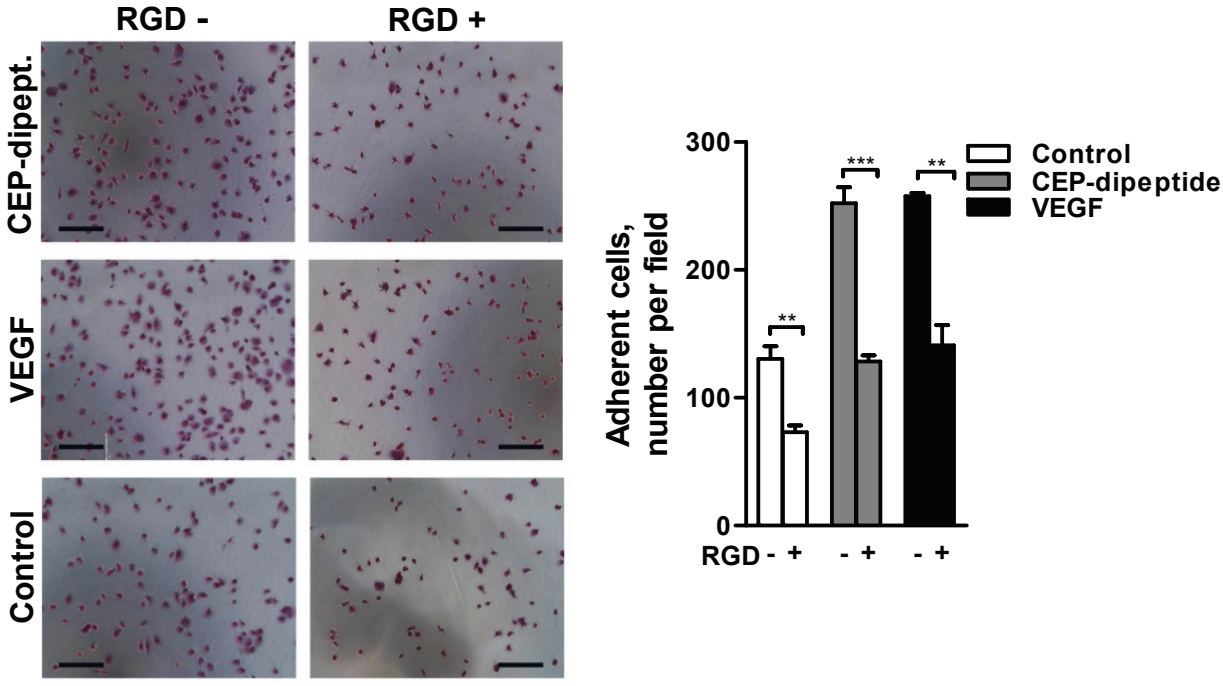

Fig.S5. a. HUVEC migration assay: Cells were treated with CEP-MSA, CEP-dipeptide, CPP-HSA or VEGF at the indicated concentration or remained untreated (control). Bars represent percent increase over control, mean ± s.e.m., n=4. *** represents p<0.001. **b.** CEP induced effects are integrin-dependent. Cell adhesion assay, Left - staining with hematoxylin; scale bars are 150 µm, CEP dipeptide treatment 0.5µg/ml, VEGF 60ng/ml. RGD peptide added at a concentration of 1.5mM where indicated. Right– average cell number calculated in six independent fields, mean ± s.e.m. ** represents p<0.01 and *** represents p<0.001 vs. RGD-.

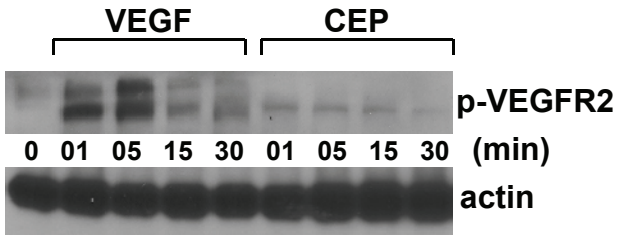

Fig.S6. The CEP adduct does not induce VEGFR2 kinase activity. HUVEC cells treated with VEGF (60ng/ml) or CEP-dipeptide (0.5µg/ml) for the indicated period of time were lysed and probed for phospho-VEGFR2 (top) or total actin (bottom).

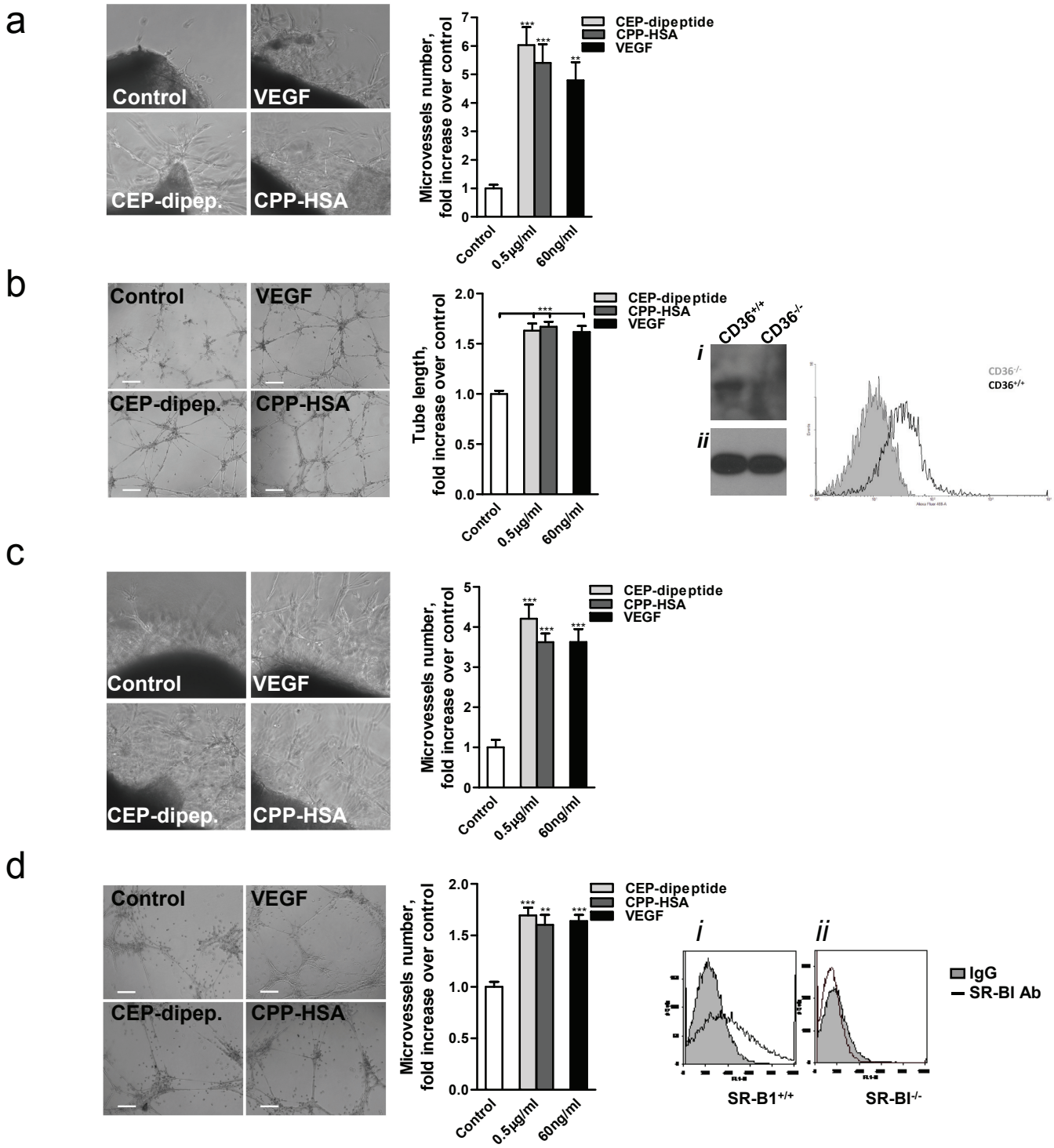

Fig.S7. Pro-angiogenic effects of the adducts are independent of CD36 and SR-BI expression. Aortic ring (**a, c**) and tube formation (**b, d**) assays using CD36 $^{-/-}$ (**a, b**) or SR-BI $^{-/-}$ (**c, d**) mice Left- representative micrographs. Right- quantification of sprouts (a,c) or tube length (b,d) stimulated by CEP-dipeptide, CPP-HSA or VEGF (positive control) as described in Methods. Bars represent fold increase over control, mean ± s.e.m., n=5. ** represents $p<0.01$ and *** represents $p<0.001$. **b.** Far right- CD36 is expressed in CD36$^{+/+}$ but not CD36$^{-/-}$ cells, both by FACS analysis and whole cell lysates probed on Western Blot with: *i* α-CD36 and *ii* α-actin antibodies. **d.** Far right- expression of SR-BI was assessed on SR-BI$^{+/+}$ (*i*) and SR-BI $^{-/-}$ (*ii*) endothelial cells by FACS analysis. Gray profile- staining with control antibodies, open profile- staining with SR-BI antibodies.

a

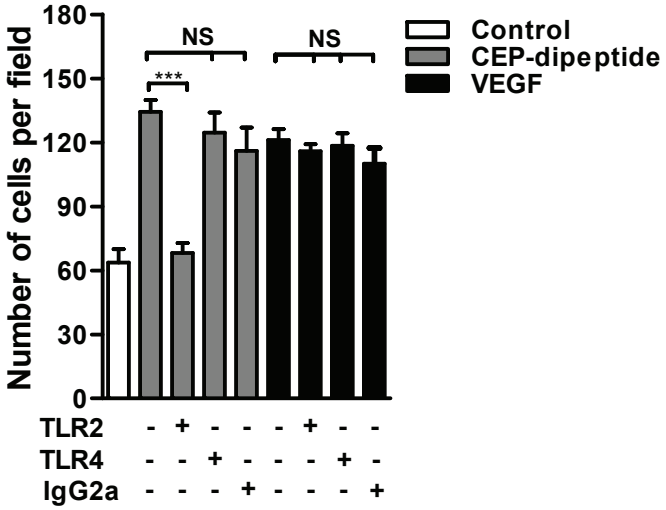

b

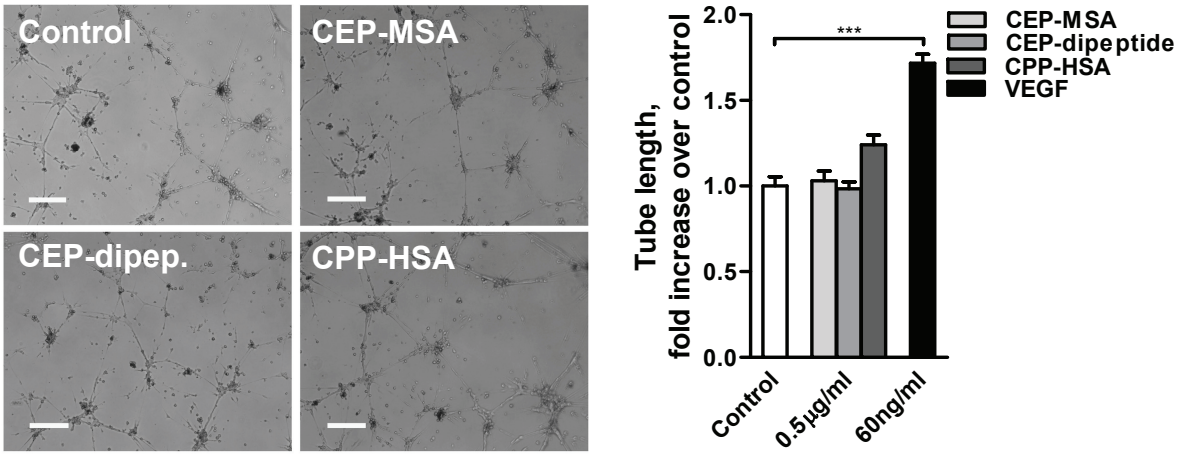

Fig.S8. CEP-induced responses are TLR2 dependent. **a.** HUVEC migration in presence of TLR2 or TLR4 blocking antibodies or non immune IgG2a antibodies as indicated. Migration assay performed as described in Methods using transwell inserts with 8 µm pore size. Bars represent average cell numbers in six fields, mean ± s.e.m. NS represents not significant differences. *** represents $p<0.001$. **b.** Oxidized adducts fail to induce angiogenesis in tube formation assay using MLEC from TLR2$^{-/-}$ mice. Left- representative micrographs of control (no treatments), CEP-MSA, CEP-dipeptide and CPP-HSA treated cells; scale bars are 200 µm. Right- bars represent fold increase in vascularization over control (no treatment) after stimulation with CEP-MSA, CEP-dipeptide, CPP-HSA or VEGF (positive control) as indicated, mean ± s.e.m., n=4. *** represents $p<0.001$.

a

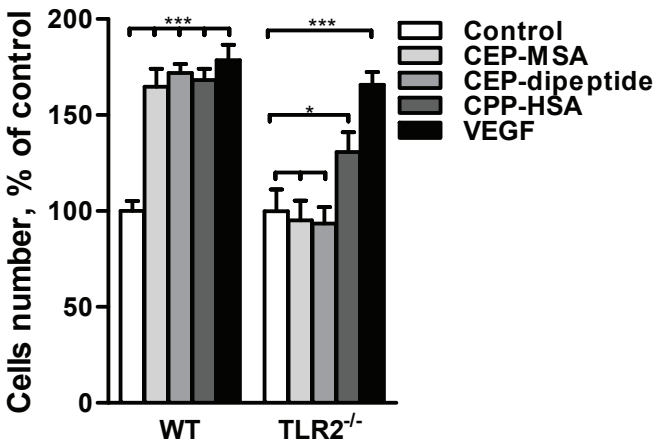

b

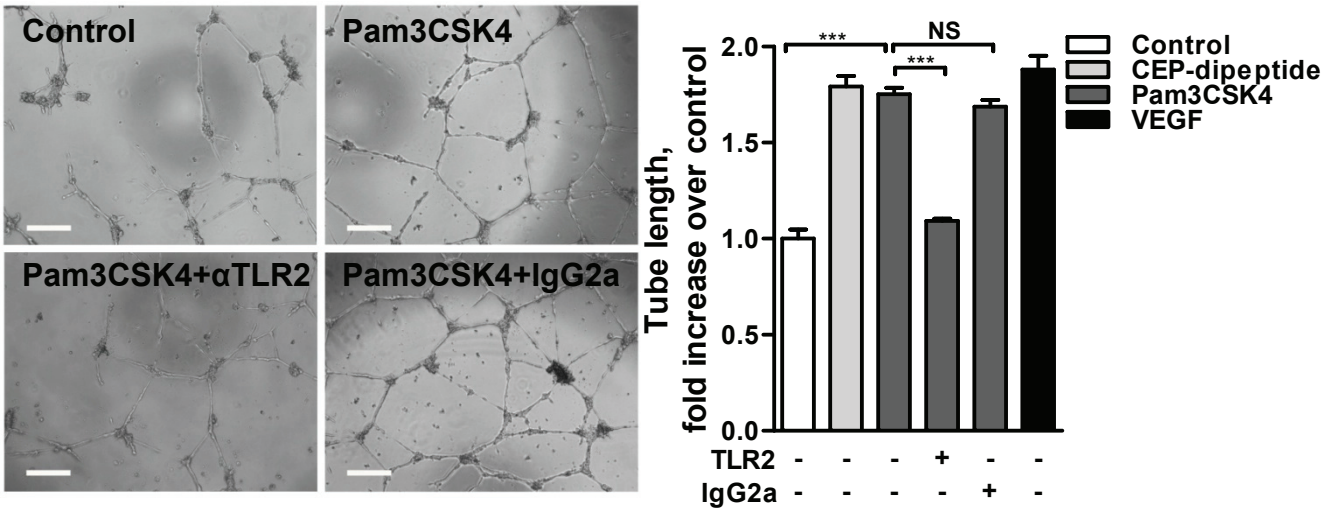

Fig.S9. a. Migration of MLEC cells in response to the adducts is dependent on TLR2 expression. Cell migration is expressed as % increase over control sample, mean ± s.e.m., n=4. * represents $p<0.05$ and *** represents $p<0.001$ vs. control. **b.** HUVEC tube formation in response to Pam3CSK4 treatment is inhibited by TLR2 blocking antibodies but not by isotype control (IgG2a) antibodies; scale bars are 200 μm. Antibodies treatment was performed as described in Methods. Right – quantification of average tube length, mean ± s.e.m., n=4. NS indicates not significant differences. *** represents $p<0.001$. CEP and VEGF-induced responses are shown for comparison.

a

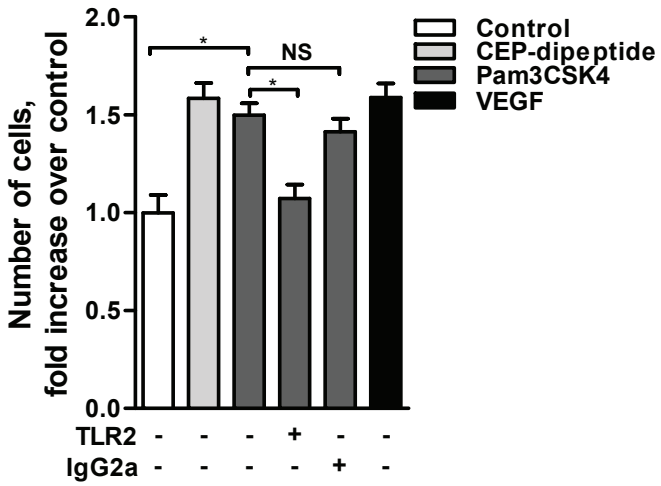

b

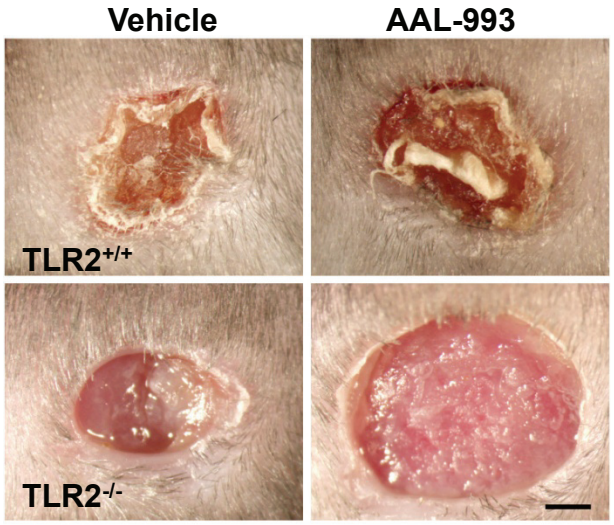

Fig.S10. a. HUVEC adhesion stimulated by Pam3CSK4 is TLR2 dependent. Cells were treated with Pam3CSK4 in the presence of absence of anti-TLR2 or isotype control (IgG2a) antibodies as indicated. Effects of CEP and VEGF are shown for comparison. Fold increase over control, mean ± s.e.m., n=4. NS represents not significant. * represents $p<0.05$. **b.** Lack of TLR2 expression and treatment with VEGFR inhibitor AAL-993 result in suppression of wound healing. Note an additive effect (right bottom image). Images of the wounds of $TLR2^{+/+}$ (top) and $TLR2^{-/-}$ animals (bottom) at day 6; after s.c. injections of AAL-993 (13nmol) or vehicle at days 0, 2, 4 and 5; scale bar is 1 mm.

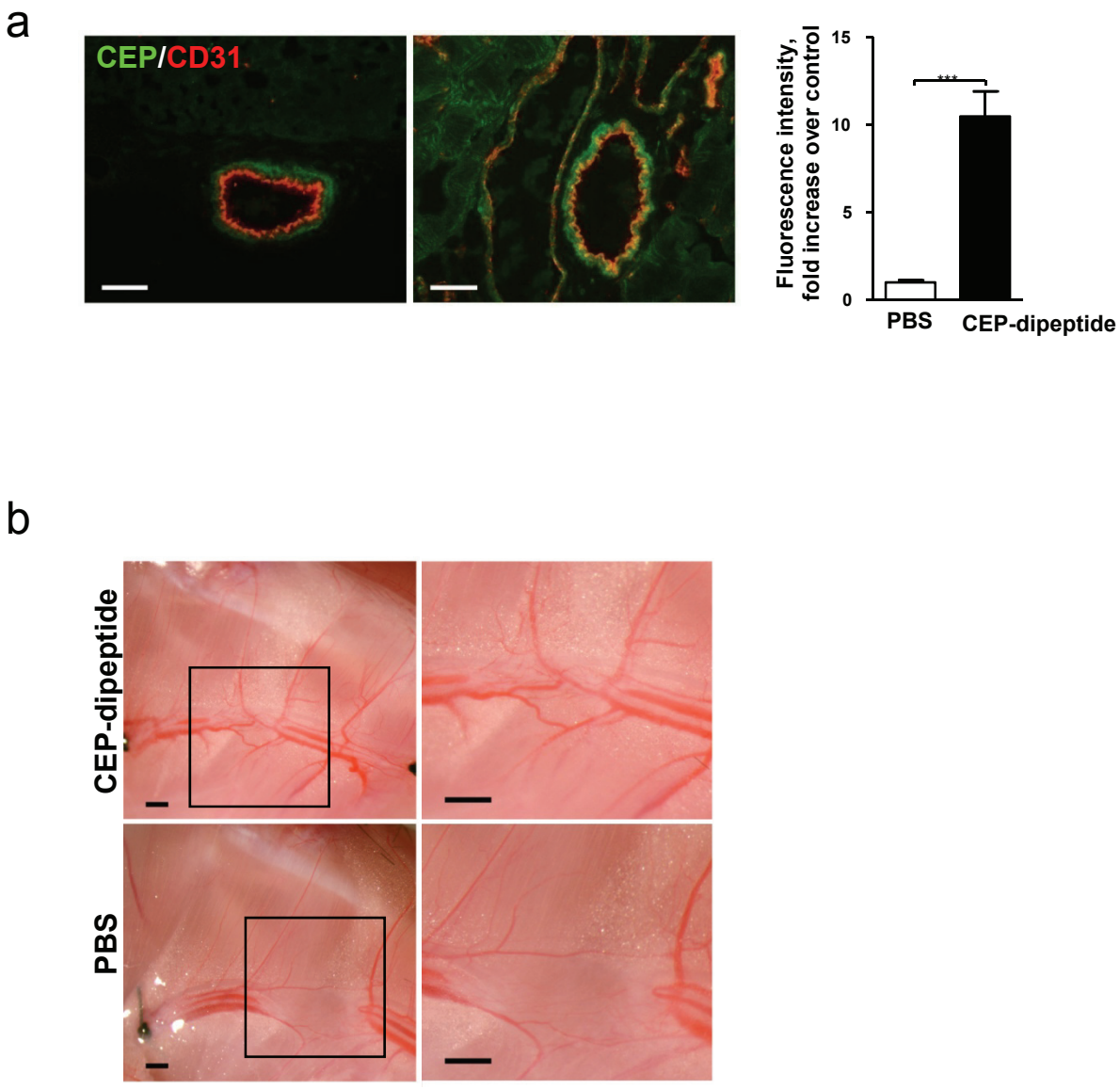

Fig.S11. a. Immunostaining of mouse hind limb muscle tissue one day after CEP-dipeptide (right) or PBS (left) injection as described in Methods. Red – CD31, green – CEP; scale bars are 40 μm. Far right- bars represent fluorescence intensity over control, mean ± s.e.m., n=5. *** represents $p<0.001$. **b.** Images of the site of femoral artery ligation from the hind limb ischemia model (described in Methods). Left- The samples was obtained at day 28 after surgery after treatment with CEP or vehicle (PBS) by intramuscular injections as indicated; scale bars are 500 μm. On the right - magnified view of the area indicated on the photograph on the left; scale bars are 500 μm.

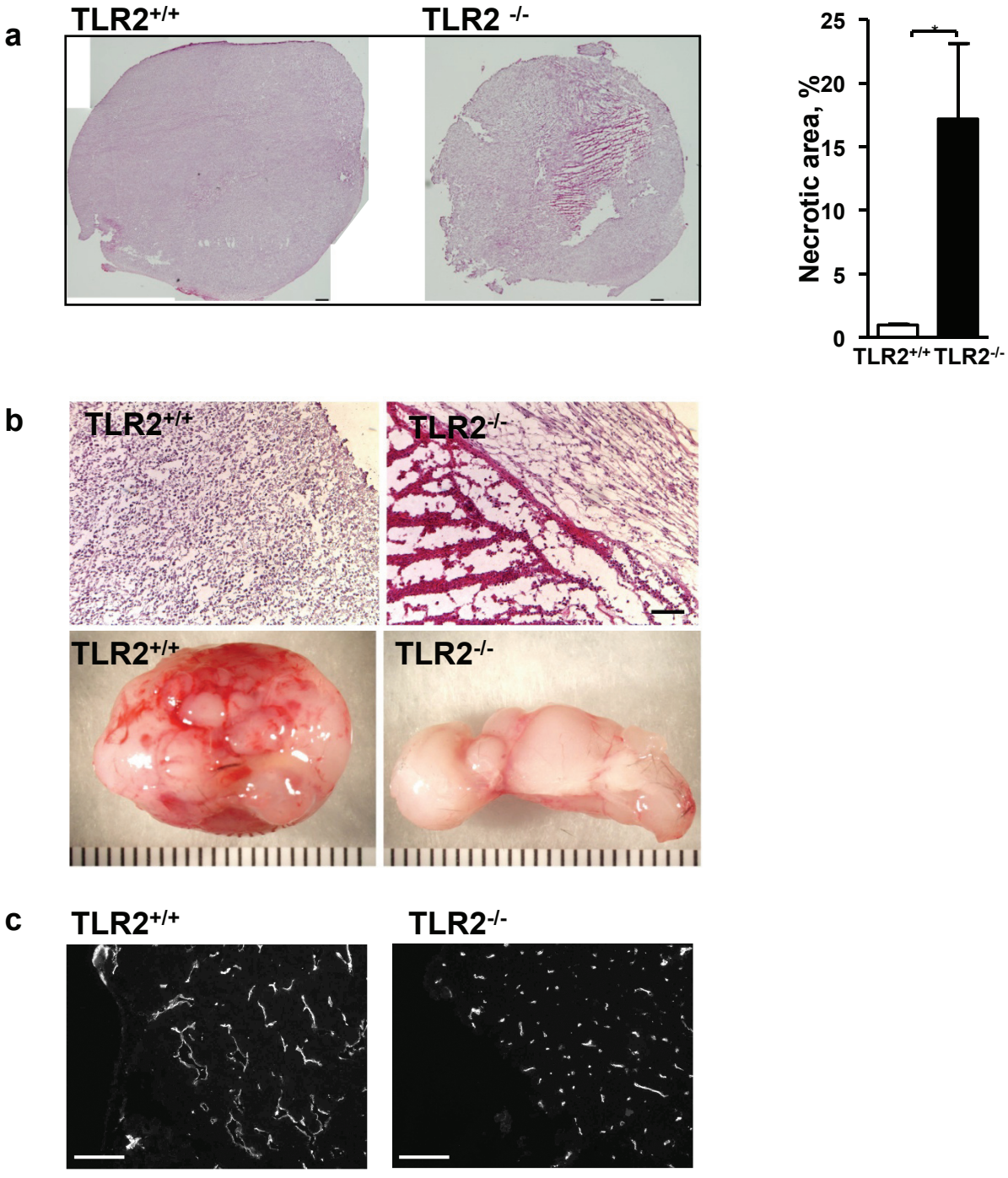

Fig.S12. TLR2$^{+/+}$ or TLR2 $^{-/-}$ mice were injected subcutaneously with 4x10^5 RM1 cells and sacrificed 12 days post implantation. **a.** Composite image of H&E staining across entire tumor; scale bar is 1 mm. Right– areas of necrosis were quantified based on H&E staining and expressed as % of total tumor area, mean ± s.e.m., n=4. * represents $p<0.05$. **b.** Top – higher magnification of tumor edge after H&E staining is shown, scale bar is 100 μm; Bottom – photographs of excised tumors; scale is 1 mm. **c.** CD31 staining of excised tumors. TLR2$^{+/+}$ - left, TLR2$^{-/-}$ -right; scale bars are 100 μm.

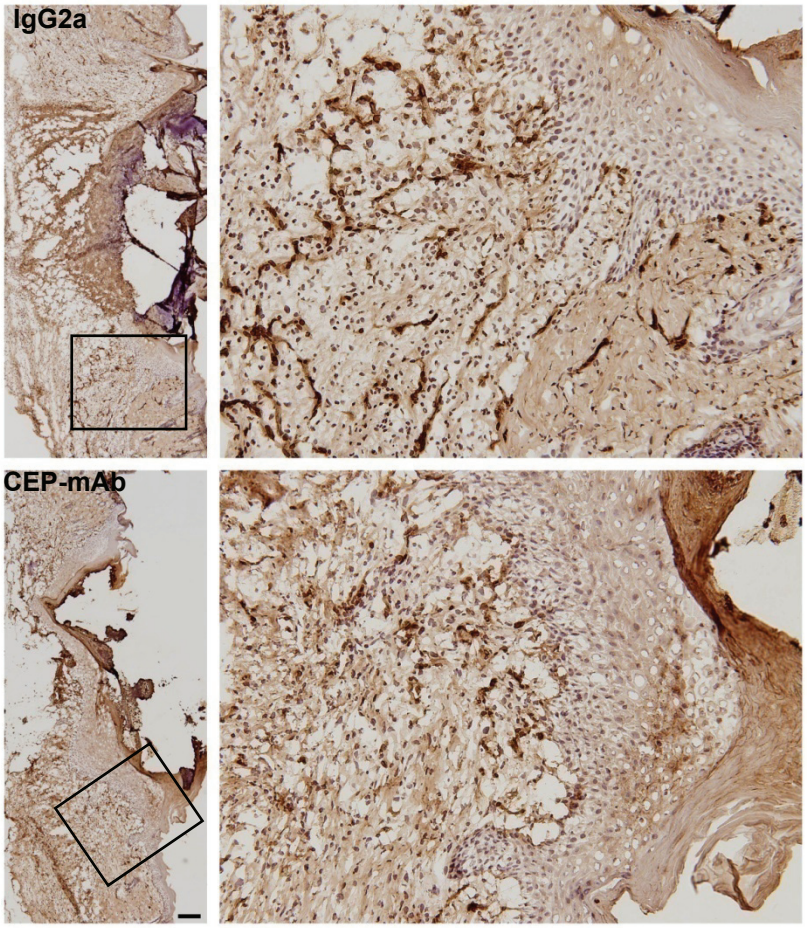

Fig.S13. Neutralization of endogenous CEP diminished vascularization of punch wounds. Prior to injury, mice were treated with control antibodies (IgG2a, top) or anti-CEP antibodies (CEP-mAb, bottom) by i.v. injections, 5μg per gram of body weight. Injections were performed 2h prior injury and every other day thereafter. After 7 days, tissues were collected, fixed and stained for CD31. Scale bar is 100 μm. Right– higher magnification image of the area indicated on the photograph on the left.

a

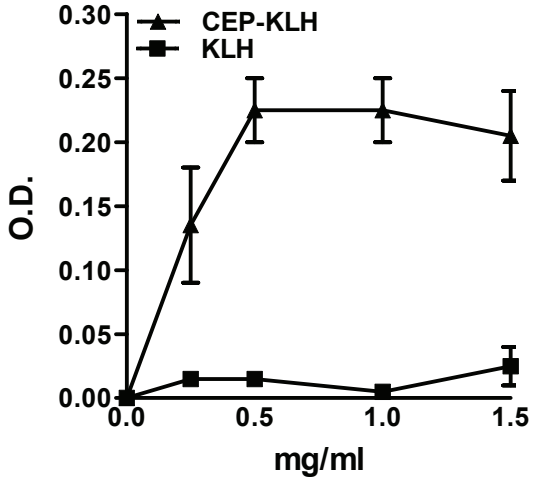

b

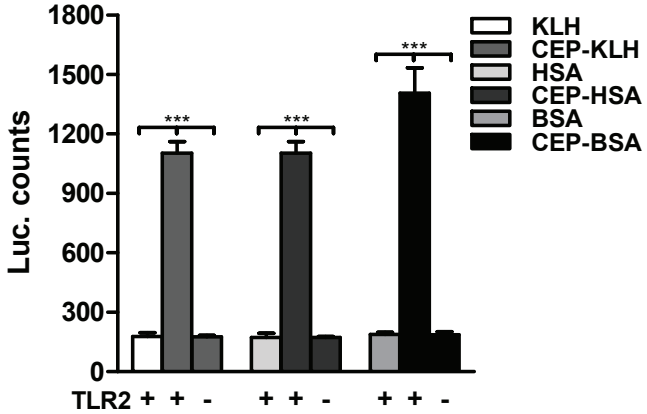

Fig.S14. **a.** TLR2 recombinant protein binding to the CEP-KLH adduct over a range of TLR2 protein concentrations. KLH protein is shown for comparison. 2µg CEP-KLH (triangles) or KLH (squares) were incubated on a 96-well polystyrene plate (Thermo Labsystems) overnight at 4°C and blocked with 5mg/ml BSA in PBS, followed by a wash with 1mg/ml BSA. We added the indicated amounts of recombinant TLR2 extracellular domain (R&D Systems) for 4h at room temperature then washed the plates. Detection was done with anti-TLR2 antibodies (clone TL2.1, eBioscience) and anti-mouse HRP-coupled antibodies (Bio-Rad). Quantification was done by a colorimetric assay (R&D Systems) at 560 nm using a Vmax plate reader (Molecular Devices). O.D. Optical density, mean ± s.e.m., n=3. **b.** A Luciferase reporter assay for NF-κB activation. TLR2 or empty vector transfection as shown on the x axis. HEK 293 cells were transfected with hTLR2 expression plasmid (InvivoGen) or control vector, as well as NF-κB luciferase reporter (gift from Dr. P. Chumakov, Cleveland Clinic). 24h post-transfection cells were exposed to CEP adduct or the carrier protein for an additional 8h. Reporter activity was measured with a luciferase assay system (Promega) and the readout was normalized to the protein content. Luciferase (Luc.) counts, mean ± s.e.m., n=3. *** represents $p<0.001$.